

Synthesis, Crystal Structure and Thermal Behaviour of the Diethylenetriammonium Oxalate–Water (1/4), $(\text{H}_3\text{dien})_2(\text{ox})_3 \cdot 4\text{H}_2\text{O}$

Pascual Román,* Carmen Guzmán-Miralles, Antonio Luque and Javier I. Beitia

Department of Inorganic Chemistry, University of País Vasco, Apartado 644, E-48080 Bilbao, Spain

Román, P., Guzmán-Miralles, C., Luque A., and Beitia, J. I., 1997. Synthesis, Crystal Structure and Thermal Behaviour of the Diethylenetriammonium Oxalate–Water (1/4), $(\text{H}_3\text{dien})_2(\text{ox})_3 \cdot 4\text{H}_2\text{O}$. – Acta Chem. Scand. 51: 13–18. © Acta Chemica Scandinavica 1997.

The compound $(\text{H}_3\text{dien})_2(\text{ox})_3 \cdot 4\text{H}_2\text{O}$ has been synthesized, chemically characterized, and its crystal structure determined by single-crystal X-ray diffraction at room temperature. It crystallizes in the triclinic system, space group $P\bar{1}$, cell dimensions $a=8.626(3)$, $b=9.361(1)$, $c=9.385(1)$ Å, $\alpha=66.02(5)$, $\beta=71.95(6)$, $\gamma=86.70(3)^\circ$, and $Z=1$. The structure was refined by full-matrix least-squares methods to $R(F_o)=0.072$ and $R_w(F_o)=0.085$. It consists of centrosymmetric and unconstrained oxalate dianions stacked in anionic ribbons which are linked together by an extensive three-dimensional hydrogen-bonding network involving the ammonium groups of the diethylenetriammonium cations and the oxygen atoms of oxalate and crystallization water molecules. The thermal behaviour of the compound has been studied by thermogravimetry (TG/DTG) and differential thermal (DTA and DSC) analysis in synthetic air and dinitrogen atmospheres. The dehydration step has been kinetically analyzed by non-isothermal methods and it is discussed on a structural basis.

In recent years, the chemistry of oxalato-containing compounds is an active area of research with interest arising from the study of the varied structural features of these compounds^{1–4} and from their applications to areas such as biological chemistry,⁵ catalysis,^{6,7} and magnetochemistry.^{8,9} In this last field, dimer and polymeric first-row transition-metal complexes with general formula $[\text{M}_x(\text{ox})_y(\text{L})_z]$ (where $\text{M}=\text{Mn}$, Fe , Co , Ni , Cu or Zn , $\text{L}=\text{aliphatic}$ or $\text{aromatic polydentate amine}$) are of particular interest to study strong exchange interactions^{10–13} and to evaluate the influence of the peripheral donor atoms on intramolecular exchange coupling.

Usually, oxalato-bridged complexes are prepared by mixing of commercially available metal(II) halide, sodium/potassium oxalate and the amine base in the appropriated molar ratio. However, in many cases, poor yields or single crystals unsuitable for X-ray studies are obtained, and non-commercially available products, such as $\text{K}_2[\text{Ni}(\text{ox})_2(\text{H}_2\text{O})_2] \cdot 4\text{H}_2\text{O}$ ¹⁴ and organoammonium oxalate, must be used. In this context, we have prepared and structurally characterized the compound $(\text{H}_3\text{dien})_2(\text{ox})_3 \cdot 4\text{H}_2\text{O}$ (**1**) (dien = diethylenetriamine and ox^{2-} = oxalate anion), which is used as a starting material in our structural and reactivity investigations on $\text{Ni}^{\text{II}}\text{-ox-L}$ mixed complexes.

* To whom correspondence should be addressed.

Experimental

Materials. Diethylenetriamine and oxalic acid dihydrate were of Merck reagent grade and were used without further purification.

Physical measurements. Carbon, nitrogen and hydrogen analyses were performed on a Perkin Elmer CHN-2400 analyser. IR spectra were recorded on a Nicolet 740 FTIR spectrophotometer in the $4000\text{--}400\text{ cm}^{-1}$ region as KBr pellets. Density value was measured by flotation in a mixture of acetone–carbon tetrachloride. A Setaram TAG 24 S 16 simultaneous thermal analyser was used to obtain the differential thermal analysis (DTA) and thermogravimetric analysis (TG and DTG) curves, in synthetic air and dinitrogen atmospheres. Calorimetric measurements were carried out on a Mettler TA 4000 DSC instrument, using synthetic air and dry dinitrogen atmospheres. All thermal decompositions were recorded at a heating rate of 5°C min^{-1} in a dynamic atmosphere with a flow rate of $50\text{ cm}^3\text{ min}^{-1}$.

Synthesis. Diethylenetriammonium oxalate tetrahydrate (**1**) was obtained by slow addition of diethylenetriamine (1.7 mL, 15.60 mmol) over an amount of oxalic acid dihydrate (2.52 g, 20.00 mmol) in aqueous solution (50 mL). Initially, a white precipitate was formed which was

dissolved progressively and a clear solution was obtained at the end of the addition. Polyhedral yellow crystals suitable for X-ray structural analysis were separated by slow evaporation at room temperature. The crystals were filtered off, washed with small amounts of cold water and dried in air. Analytical data: Calculated for $C_{14}H_{40}N_6O_{16}$: C, 30.66; H, 7.35; N, 15.32. Found: C, 30.74; H, 7.44; N, 15.41%. The number of crystallization water molecules was determined thermogravimetrically. IR data (KBr pellets, cm^{-1}): 3490br and 3410br (ν OH), 3500–2700s (ν NH), 1600vs, 1510w, 1485w and 1455w (δ NH), 1600vs (ν_{as} O–C–O), 1430w and 1405w (δ CH₂), 1345s and 1310s (ν_s O–C–O), 1200–950m (ω , γ , ρ CH₂), 1135m, 985w and 860w (ν C–C_{ox}), 800w and 720w (γ NH and δ O–C–O), 520m (δ C–C–O) and 480w (ρ O–C–O).

Crystallographic data collection and structure determination. A single crystal of size $1.00 \times 0.78 \times 0.42$ mm of **1** was selected and mounted on an Enraf–Nonius CAD4 four-circle diffractometer. Accurate unit-cell parameters were determined from automatic centring of 25 strong reflections ($7 \leq \theta \leq 14$) and refined by a least-squares method. Intensity data collection was carried out at room temperature using graphite monochromatized Mo-K α radiation (0.71069 Å) and operating in the $\omega/2\theta$ scan mode. Crystallographic data, conditions retained for the intensity data collection, and some features of the structure refinement are summarized in Table 1.

The intensity of two reference reflections were monitored every 100 reflections and 3600 s. No intensity losses were observed during the data collection process. A total of 3816 unique reflections were recorded in the range $2 \leq 2\theta \leq 60^\circ$; 2846 of which, with $I \geq 3\sigma(I)$, were assumed as observed and used in the refinement. The intensity data were corrected for Lorentz and polarization effects but no absorption correction was applied. The atomic scattering factors and anomalous dispersion factors were taken from Ref. 15. The structure was solved by automatic direct methods¹⁶ and refined by full-matrix least-squares analysis using the X-RAY76 System.¹⁷ After refinement of positional and anisotropic thermal parameters for non-hydrogen atoms, the positions of the hydrogen atoms were located on a difference Fourier map and refined isotropically, except those bonded to the oxygen water molecules which were included at calculated sites and refined as fixed contributors ($U = 0.05 \text{ \AA}^2$). After the final refinement cycle, the agreement factors were $R(F_o) = 0.072$ and $R_w(F_o) = 0.085$, 227 variables, $S = 1.20$, $(\Delta/\sigma)_{\max} = 0.145$, $(\Delta/\sigma)_{\text{av}} = 0.010$, and $\Delta\rho_{\max} = 0.36 \text{ e \AA}^{-3}$.

Final atomic coordinates and equivalent isotropic thermal parameters for non-H atoms are given in Table 2, while selected bond distances and angles are listed in Table 3.

Table 1. Crystal data, intensity collection and structure refinement for $(H_3dien)_2(ox)_3 \cdot 4H_2O$.

Formula	$C_{14}H_{40}N_6O_{16}$
Formula weight/g mol ⁻¹	548.50
Crystal system	Triclinic
Space group	$P\bar{1}$
<i>a</i> /Å	8.626(3)
<i>b</i> /Å	9.361(1)
<i>c</i> /Å	9.385(1)
α /°	66.02(5)
β /°	71.95(6)
γ /°	86.70(3)
<i>V</i> /Å ³	656.3(2)
<i>Z</i>	1
μ (λ Mo K α)/cm ⁻¹	1.177
ρ (calcd), ρ (obs)/g cm ⁻³	1.39, 1.40(1)
Crystal size/mm	$1.00 \times 0.78 \times 0.42$
Habit	Rhombic prism
Color	Yellow
<i>F</i> (000)	294
Scan range/°	$1 \leq \theta \leq 30$
Scan width/°	$\Delta\theta = 1.0 + 0.35 \tan \theta$
Scan method	$\omega/2\theta$
<i>hkl</i> range	$0 \leq h \leq 12$; $-13 \leq k \leq 13$; $-13 \leq l \leq 13$
Standard reflections	2 measured every 100 reflections
Variation in standard intensities	<2%
Reflections collected	3816
Reflections observed (<i>n</i>)	2846 [$I \geq 3\sigma(I)$]
No. of variables (<i>m</i>)	227
<i>S</i> ^a	1.20
$\Delta\rho_{\max}/\text{e \AA}^{-3}$	0.36
Δ/σ_{\max} (non-H)	0.018 [<i>U</i> ₁₁ of N(1)]
Δ/σ_{\max} (H)	0.145 [γ of H(22)]
$\Delta/\sigma_{\text{ave}}$	0.010
<i>R</i> (<i>F</i>) ^b / <i>R</i> _w (<i>F</i>) ^c	0.072/0.085

$$^a S = [\sum w(F_o - F_c)^2 / (n - m)]^{1/2}. \quad ^b R = \sum (|F_o| - |F_c|) / \sum |F_o|. \quad ^c R_w = \sum (|F_o| - |F_c|)_w^{1/2} / \sum |F_o|_w^{1/2}.$$

Table 2. Final fractional coordinates and equivalent temperature factors with estimated standard deviations for non-H atoms.

Atom	<i>x/a</i>	<i>y/b</i>	<i>z/c</i>	<i>U</i> _{eq} ^a
O(10)	0.1242(2)	0.1495(2)	-0.0777(2)	454(9)
O(20)	0.3888(3)	0.1702(4)	-0.1066(4)	802(18)
O(30)	0.3226(2)	0.3539(2)	0.0651(2)	436(9)
O(40)	0.0588(2)	0.2685(2)	0.1548(2)	467(9)
C(10)	0.2440(3)	0.1928(3)	-0.0504(3)	333(8)
C(20)	0.2047(2)	0.2799(2)	0.0667(3)	292(7)
O(11)	0.5088(2)	0.3508(2)	0.4283(3)	471(9)
O(21)	0.6874(2)	0.4250(2)	0.5208(2)	451(9)
C(11)	0.5566(2)	0.4352(3)	0.4842(2)	316(8)
N(1)	0.6459(2)	0.4033(2)	-0.1584(2)	309(7)
C(2)	0.7500(3)	0.2804(3)	-0.0847(3)	349(8)
C(3)	0.6875(3)	0.2215(3)	0.0997(3)	347(8)
N(4)	0.7943(2)	0.1022(2)	0.1745(2)	286(7)
C(5)	0.7259(3)	0.0282(3)	0.3571(3)	388(9)
C(6)	0.8366(3)	-0.0892(3)	0.4370(3)	401(10)
N(7)	0.8257(3)	-0.2424(2)	0.4237(3)	375(8)
O(01) _w	1.0066(2)	0.4158(2)	0.3634(2)	420(8)
O(02) _w	0.6821(4)	0.0726(3)	0.7010(3)	786(15)

$$^a U_{\text{eq}} = (1/3) \sum [U_{ij} a_i^* a_j^* a_i a_j \cos(a_i, a_j)] (\text{\AA}^2 \times 10^4).$$

Table 3. Bond distances (in Å), bond angles (in °) and dihedral angles (in °) with estimated standard deviations for non-hydrogen atoms.

C(10)–O(10)	1.263(4)	C(11)–C(11) ⁱ	1.578(5)
C(10)–O(20)	1.239(3)	N(1)–C(2)	1.492(3)
C(20)–O(30)	1.256(3)	C(2)–C(3)	1.507(3)
C(20)–O(40)	1.256(2)	C(3)–N(4)	1.495(3)
C(10)–C(20)	1.566(4)	N(4)–C(5)	1.490(3)
C(11)–O(11)	1.255(4)	C(5)–C(6)	1.528(4)
C(11)–O(21)	1.265(3)	C(6)–N(7)	1.500(4)
O(10)–C(10)–O(20)	125.4(3)	O(21)–C(11)–C(11) ⁱ	115.9(2)
C(20)–C(10)–O(20)	117.7(3)	O(11)–C(11)–C(11) ⁱ	118.0(2)
O(10)–C(10)–C(20)	116.9(2)	N(1)–C(2)–C(3)	109.6(2)
C(10)–C(20)–O(40)	117.3(2)	C(2)–C(3)–N(4)	110.1(2)
C(10)–C(20)–O(40)	116.9(2)	C(3)–N(4)–C(5)	111.6(2)
O(30)–C(20)–O(40)	125.8(2)	N(4)–C(5)–C(6)	112.6(2)
O(11)–C(11)–O(21)	126.1(3)	C(5)–C(6)–N(7)	112.5(2)
N(1)–C(2)–C(3)–N(4)	178.1(2)	C(3)–N(4)–C(5)–C(6)	177.5(2)
C(2)–C(3)–N(4)–C(5)	173.6(2)	N(4)–C(5)–C(6)–N(7)	76.9(3)

Symmetry code: (i) $-x+1, -y+1, -z+1$.

Results and discussion

Description of the structure. The crystal structure of compound **1** is made up of diethylenetriammonium cations, $(\text{H}_3\text{dien})^{3+}$, centrosymmetric oxalate dianions with an inversion centre in the middle of the C–C bond, crystallographic unconstrained oxalate anions, and water molecules. A perspective view of these units, with the atom-numbering scheme, is depicted in Fig. 1. The structural units are held together by means of electrostatic forces and an extensive three-dimensional network of

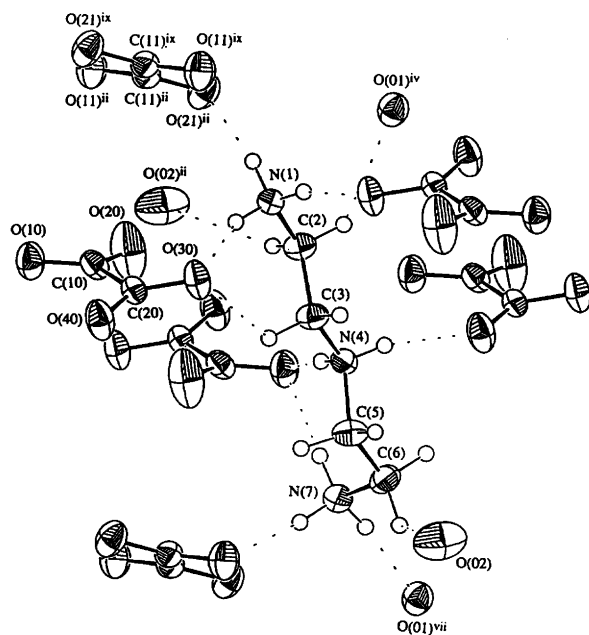


Fig. 1. Structural units of $(\text{H}_3\text{dien})_2(\text{ox})_3 \cdot 4\text{H}_2\text{O}$ showing the atomic labelling and some of the hydrogen bond interactions. Symmetry code ix: $-x+1, -y+1, -z+2$. See Table 4 for other symmetries.

hydrogen bonds, most of them being represented by broken lines in Fig. 1.

In contrast with the centrosymmetric oxalate, the planarity of which is imposed by the inversion centre, the unconstrained oxalate deviates significantly from planarity and shows a dihedral twist around the C–C bond of $16.7(1)^\circ$. Bond distances and angles in both anions (Table 3) are in the range reported for analogous oxalate compounds.^{18–20} However, it is interesting to note the effects of the hydrogen bonds on the carbon–oxygen bonds lengths. This influence is clearly visible in the non-symmetric oxalate. The bond distance C(10)–O(20) [1.239(3) Å] is shorter than the other three C–O ones [mean 1.258(4) Å]. The O(20) atom only accepts a hydrogen bond from a water molecule, whereas the other three oxygen atoms receive two hydrogen contacts (Table 4).

The bond distances and angles of the diethylenetriammonium cation are as expected.^{21–23} The cation shows a *trans* (178.1°)–*trans* (173.6°)–*trans* (177.5°)–*gauche* (76.9°) conformation with the terminal nitrogen atom, N(7), 1.30 Å out of the mean plane passing through the rest of the atoms.

In the crystal structure (Fig. 2), the oxalate dianions form infinite ribbons along the [111] direction with a sequence $\text{ox}_s\text{--ox}_{ns}\text{--ox}_{ns}\text{--ox}_s$ (where *s* = centrosymmetric and *ns* = non-centrosymmetric) and with a dihedral angle between the oxalate mean planes of $36.18(7)^\circ$.

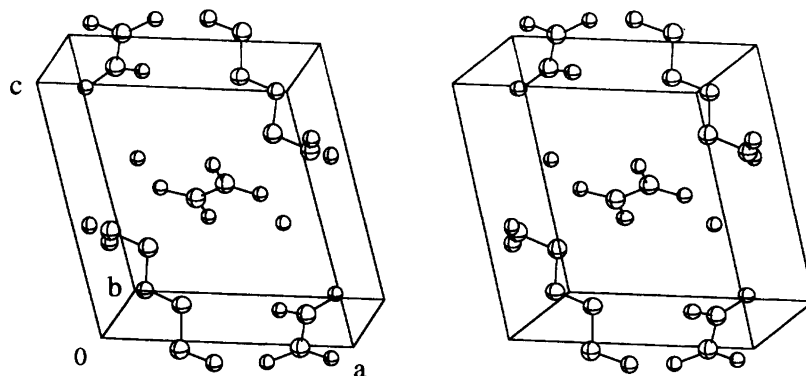
The diethylenetriammonium cations are stacked between the anionic ribbons and oriented nearly perpendicular to them [$\text{dien} \wedge \text{ox}_{ns} = 72.3(1)^\circ$ and $\text{dien} \wedge \text{ox}_s = 68.6(1)^\circ$]. The two $-\text{NH}_3$ groups at the end of the organic chain form strong $\text{N–H} \cdots \text{O}$ hydrogen-bond with the two oxalate moieties, whereas the central ammonium group establishes two hydrogen bonds involving oxygen atoms from two adjacent centrosymmetric oxalate anions. The three-dimensional hydrogen-bond network

Table 4. Hydrogen-bonding system (in Å, °).

D-H...A	D-H	D...A	H...A	<D-H...A
N(1)-H(11)...O(30)	0.93(3)	2.851(2)	1.98(3)	153(3)
N(1)-H(12)...O(21) ⁱⁱ	0.95(4)	2.842(3)	1.90(5)	169(3)
N(1)-H(13)...O(30) ⁱ	0.91(5)	2.800(3)	1.91(6)	165(3)
C(2)-H(21)...O(01) _w ^{iv}	1.00(4)	3.252(3)	2.49(3)	133(3)
C(2)-H(22)...O(02) _w ⁱⁱ	0.96(4)	3.495(5)	2.63(5)	150(3)
N(4)-H(41)...O(10) ^v	0.92(4)	2.833(3)	1.92(3)	172(3)
N(4)-H(42)...O(40) ⁱⁱⁱ	0.87(4)	2.752(3)	1.93(5)	158(4)
C(6)-H(62)...O(02) _w	1.04(4)	3.313(4)	2.60(5)	125(2)
N(7)-H(71)...O(11) ^{vi}	0.96(3)	2.827(3)	1.87(3)	174(3)
N(7)-H(72)...O(01) _w ^{vii}	0.94(4)	2.758(3)	1.84(4)	164(3)
N(7)-H(73)...O(10) ^v	1.00(5)	2.892(3)	1.90(4)	168(4)
O(01) _w -H(011)...O(21)	0.93(-)	2.707(3)	1.79(-)	168(-)
O(01) _w -H(012)...O(40) ⁱⁱⁱ	0.94(-)	2.741(4)	1.84(-)	159(-)
O(02) _w -H(021)...O(20) ^{viii}	1.08(-)	2.956(4)	1.94(-)	156(-)
O(02) _w -H(022)...O(21)	1.05(-)	3.030(3)	2.00(-)	165(-)

Symmetry codes:

(i) $-x+1, -y+1, -z$; (ii) $x, y, z-1$; (iii) $x+1, y, z$; (iv) $-x+2, -y+1, -z$; (v) $-x+1, -y, -z$; (vi) $-x+1, -y, -z+1$; (vii) $-x+2, -y, -z+1$; (viii) $x, y, z+1$.

Fig. 2. Stereoscopic representation of $(\text{H}_3\text{dien})_2(\text{ox})_3 \cdot 4\text{H}_2\text{O}$ showing the molecular arrangement.

is completed with the water molecules, which are placed in the interstitial spaces between the anions and cations. The first water molecule, $\text{O}(01)_w$, donates two short hydrogen bonds to oxygen atoms from the oxalate anions and accepts a strong $\text{N}-\text{H} \cdots \text{O}$ contact from a terminal NH_3 group of the cation. This water molecule completes its distorted tetrahedral hydrogen-bond environment with a $\text{C}-\text{H} \cdots \text{O}_w$ contact involving an ethylene group of the organic cation.

In a recent study of the $\text{C}-\text{H} \cdots \text{O}_w$ hydrogen bond in 46 neutron crystal structures, Steiner and Saenger²⁴ have found that water molecules prefer to accept strong hydrogen bonds from OH and NH donors, but if these are not available in a suitable configuration, it will resort to the weaker $\text{C}-\text{H} \cdots \text{O}_w$ hydrogen bonds rather than leaving its multiple acceptor potential unsatisfied. The role of $\text{C}-\text{H} \cdots \text{O}$ has long been known to spectroscopists and crystallographers,^{25,26} but definitive evidence for its structural significance was given only a few years ago in biological macromolecular structures and smaller organic systems.²⁷

The $\text{O}(02)_w$ water molecule forms two strong

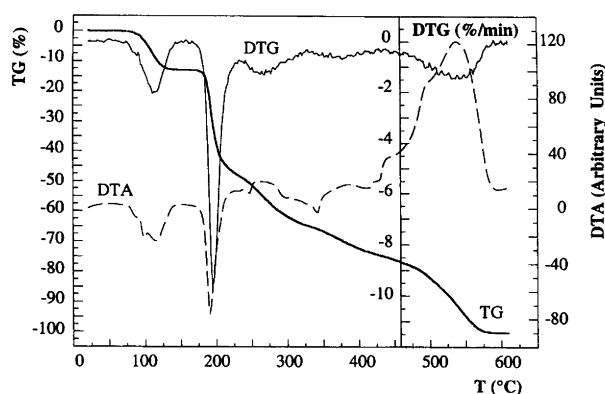
$\text{O}_w-\text{H} \cdots \text{O}$ hydrogen bonds and it satisfies all its acceptor potential with two weak $\text{C}-\text{H} \cdots \text{O}_w$ hydrogen bonds. Consequently, the hydrogen bond environment of this water molecule is weaker than that above described for $\text{O}(01)_w$. This fact may explain the high thermal motion of the $\text{O}(02)_w$, which would be presumably the first molecule released during the thermal dehydration process.

Thermal behaviour. Thermal evolution of the compound was studied under synthetic air and dinitrogen atmospheres (Fig. 3). The thermoanalytical data are shown in Table 5. In both atmospheres, the thermal degradation starts with the loss of the crystallization water molecules during an endothermic process in the range 70–145 °C. Although TG curves show a single step for the dehydration process, DTG and DTA curves reveal that this process takes place in three successive steps. The two first ones are almost overlapped, and the mass loss corresponds to the cleavage of two water molecules. The third step involves the loss of the remaining two water molecules. This fact is in accordance with the X-ray

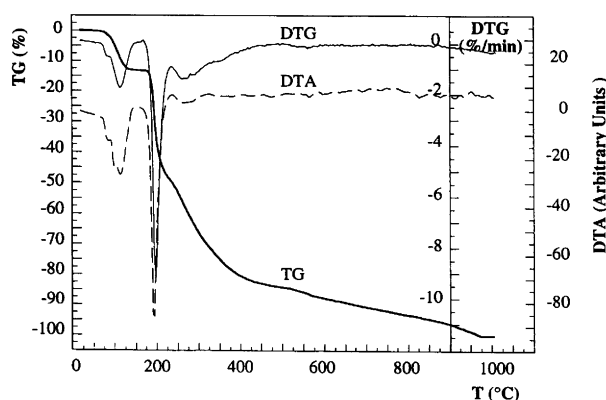
Table 5. Thermoanalytical data for the decomposition of $(\text{H}_3\text{dien})_2(\text{ox})_3 \cdot 4\text{H}_2\text{O}$ in synthetic air and dinitrogen atmospheres.

Process	Synthetic air			Dinitrogen		
	$\Delta T^\circ/\text{C}$	Δm (%)	Δm_{theor} (%)	$\Delta T/\text{C}$	Δm (%)	Δm_{theor} (%)
Dehydr.	70–145(–)	12.98	13.13	70–145(–)	13.13	13.13
Decomp.	170–230(–)	34.99		170–230(–)	35.87	
Decomp.	230–590(+)	52.03		230–970 ^b	51.00	

^aEndothermic (–) or exothermic (+) process. ^bProgressive mass loss without clear peaks in DTG and/or DTA curves.



(a)



(b)

Fig. 3. Thermal decomposition of $(\text{H}_3\text{dien})_2(\text{ox})_3 \cdot 4\text{H}_2\text{O}$ in (a) synthetic air and (b) dinitrogen atmospheres.

structural determination, which shows that the crystallographically independent water molecules present quite different hydrogen-bonding environments. The total dehydration process has been studied by means of non-isothermal kinetic analysis²⁸ using 21 theoretical models. In both atmospheres, the best fit corresponds to an 'order of reaction 1' model [$f(\alpha) = -\ln(1-\alpha)$] with activation energies of 96 [air] and 88 [dinitrogen] kJ mol^{-1} , indicating that this step is a decelerating process. The dehydration enthalpies of 253 [air] and 212 [N_2] kJ mol^{-1} , as determined by the DSC curves, are in good agreement with the values reported previously for other crystal hydrates ($\Delta H = 50\text{--}65 \text{ kJ mol}^{-1} \text{ H}_2\text{O}$).^{29,30}

Once the compound is dehydrated, it undergoes decomposition in two stages. The first one is endothermic and occurs in the range 170–230 °C. The residues obtained in this process were analyzed by means of IR spectroscopy and elemental analysis. The spectrum at 230 °C exhibited bands at 3235s, 1675vs, 1620m, 1355w, 1040w, 670m, 465w cm^{-1} , which agree with those of free oxamide,³¹ together with some additional peaks which could not be assigned. Some authors have suggested that the thermal decomposition of organic oxalates^{32,33} leads to an intermediate residue which could be a mixture of oxamide, or a product with $-\text{NH}-\text{CO}-\text{CO}-\text{NH}-$ structure, and a carbonaceous residue. The thermal degradations finish with the total mass loss of the compound at 590 and 970 °C in air and dinitrogen atmosphere, respectively.

Acknowledgements. This work was supported by UPV/EHU (grant no. UPV 169.310-EA134/95). C. G.-M. acknowledges financial support from Departamento de Educación del Gobierno Vasco (grant no. BFI90.062 Modalidad BE).

Supplementary material available from the authors. Tables of crystallographic data, thermal parameters for non-hydrogen atoms, hydrogen coordinates, and a listing of bond lengths, bond angles, inter- and intramolecular contacts including hydrogen contacts (9 pp.); a listing of the observed and calculated structure factors (16 pp.).

References

- Escuer, A., Vicente, R., Ribas, J., Jaud, J. and Raynaud, B. *Inorg. Chim. Acta* 216 (1994) 139.
- De Munno, G., Julve, M., Nicolo, F., Lloret, F., Faus, J., Ruiz, R. and Sinn, E. *Angew. Chem., Int. Ed. Engl.* 32 (1993) 613.
- Farrell, R. P., Hambley, T. W. and Lay, P. A. *Inorg. Chem.* 34 (1995) 757.
- Decurtins, S., Schmalle, H. W., Schneuwly, P., Ensling, J. and Gülich, P. *J. Am. Chem. Soc.* 116 (1994) 9521.
- Cleare, M. J. *Coord. Chem. Rev.* 12 (1974) 349.
- Díaz-Guemes, M. I., Bhatti, A. S. and Dollimore, D. *Thermochim. Acta* 110 (1987) 275.
- Sinha, A. and Shankar, V. *Ind. Eng. Chem. Res.* 32 (1993) 1061.
- De Munno, G., Ruiz, R., Lloret, F., Faus, J., Sessoli, R. and Julve, M. *Inorg. Chem.* 34 (1995) 408.
- Decurtins, S., Schmalle, H. W., Schneuwly, P. and Oswald, H. R. *Inorg. Chem.* 32 (1993) 1888.
- Oshio, H. and Nagashima, U. *Inorg. Chem.* 31 (1992) 3295.

11. Gleizes, A., Julve, M., Verdaguer, M., Real, J. A., Faus, J. and Solans, X. *J. Chem. Soc., Dalton Trans.* (1992) 3209.
12. Glerup, J., Goodson, P. A., Hodgson, D. J. and Michelsen, K. *Inorg. Chem.* 34 (1995) 6255.
13. Román, P.; Guzmán-Miralles, C.; Luque, A., Beitia, J. I., Cano, J., Lloret, F., Julve, M. and Alvarez, S. *Inorg. Chem. In press.*
14. Román, P., Guzmán-Miralles, C. and Luque, A. *Acta Crystallogr., Sect. C* 49 (1993) 1336.
15. *International Tables for X-Ray Crystallography*, Kynoch Press, Birmingham 1974, Vol IV.
16. Beurkens, P. T., Doesburg, H. M., Gould, R. O., Van der Hark, T. E. M., Prock, P. A. J., Noordik, J. H., Beurskens, G. and Parthasarathi, V. The DIRDIF program system. Technical Report of the Crystallography Lab., Tournooiveld 6525 ED, Nijmegen, The Netherlands 1982.
17. Stewart, J. M., Machin, P. A., Dickinson, C. W., Ammon, H. L., Heck, H. and Flack, H. The X-RAY76 System. Tech. Rep. TR-446. Computer Science Center, University of Maryland, College Park, MD 1976.
18. Adams, J. M. and Pritchard, R. G. *Acta Crystallogr., Sect. B* 32 (1976) 2438.
19. Newkome, G. R., Theriot, K. J. and Fronczek, F. R. *Acta Crystallogr., Sect. C* 41 (1985) 1642.
20. Reed, D. A. and Olmstead, M. M. *Acta Crystallogr., Sect. B* 37 (1981) 938.
21. Bdiri, M. and Jouini, A. *Eur. J. Solid State Inorg. Chem.* 26 (1989) 585.
22. Kamoun, S., Jouini, A., Daoud, A. *C. R. Acad. Sci., Ser. 2* 310 (1990) 733.
23. Román, P., Macías, R., Luque, A. and Gutiérrez-Zorrilla, J. M. *Mater. Res. Bull.* 27 (1992) 573.
24. Steiner, T. and Saenger, W. *J. Am. Chem. Soc.* 115 (1993) 4540.
25. Taylor, R. and Kennard, O. *J. Am. Chem. Soc.* 104 (1982) 5063.
26. Desiraju, G. R. *Acc. Chem. Res.* 24 (1991) 290.
27. Subramanian, S. and Zaworotko, M. J. *Coord. Chem. Rev.* 137 (1994) 357.
28. Satava, V. *Thermochim. Acta* 2 (1971) 423.
29. Dei, L., Guarini, G. G. T. and Piccini, S. *J. Therm. Anal.* 29 (1984) 755.
30. Giusti, J., Guarini, G. G. T., Menabue, L. and Pellacani, G. C. *J. Therm. Anal.* 29 (1984) 639.
31. Pouchert, C. J. *The Aldrich Library of FT-IR Spectra*, Aldrich Chemical, Milwaukee, WI, 1985.
32. Udupa, M. R. *Thermochim. Acta* 52 (1982) 367.
33. Gajapathy, D., Govindarajan, S. and Patil, K. C. *Thermochim. Acta* 60 (1983) 87.

Received January 22, 1996.